Inhomogeneous stretch induced patterning of molecular orientation in liquid crystal elastomers

Chihyung Ahn [a], Xudong Liang [b], Shengqiang Cai [a,b,*]

[a] *Materials Science and Engineering Program, University of California, San Diego, La Jolla, CA 92093, USA*
[b] *Department of Mechanical and Aerospace Engineering, University of California, San Diego, La Jolla, CA 92093, USA*

ARTICLE INFO

ABSTRACT

Liquid crystal elastomer (LCE) is soft active material, which can have large deformation when subjected to various external stimuli. Due to the coupling between the orientation of liquid crystal (LC) molecules in the elastomer and the deformation of LCEs, mechanical behaviors of LCEs can be significantly modified by manipulating LC molecular orientation field in the material. In the letter, we demonstrate, for the first time, that inhomogeneous and anisotropic stretch field can be used to pattern LC molecular orientation in the LCE during its synthesis. We further show that different active deformation modes can be realized in LCE sheets with different patterns of LC molecules. The method developed in the letter to pattern LC molecular orientation field in the LCE is facile and effective, which may find wide applications in fabricating programmable materials and structures.

© 2015 Elsevier Ltd. All rights reserved.

1. Introduction

A combination of liquid crystal (LC) and polymer network can form a new material-liquid crystal elastomer (LCE). The special molecular combination endows LCE with many unique properties such as soft or semi-soft elasticity [1–4] and multi-responsiveness [5–9], which have led to myriad applications ranging from artificial muscle [7,10] to stretchable optical devices [11–14]. Recently, several biological materials such as actin filament network [15] and fibrillar collagens [16] have also been found to have similar molecular structure and behaviors as man-made LCEs.

A salient feature of LCE is that the orientation of LC molecules inside the elastomer is coupled with macroscopic deformation of polymer network and vice versa [17–21]. In another word, the change of the orientation of LC molecules can deform the elastomer. On the other hand, the deformation of the elastomer can induce reorientation of LC molecules. As a consequence, LC molecules with macroscopically uniform orientation (or monodomain LCE) can be achieved by applying uniaxial stretch onto a polydomain LCE sample, which has been utilized to synthesize monodomain LCEs as first developed by Finkelmann et al. [22]. In the experiment, uniaxial tension was applied onto a lightly-crosslinked polydomain LCE sample to align the LC molecules in one direction. The aligned orientation of LC molecules was further frozen in the LCE by the second-step crosslinking of the polymer network. The development of the synthesis of monodomain LCE has greatly broadened its applications [23,24]. The method developed by Finkelmann is still commonly adopted by different researchers to make monodomain LCE due to its robustness and generality.

Because of the coupling between the orientation of LC molecules and the network deformation, deformation of LCEs can be driven by various external stimuli such as temperature change, light irradiation and magnetic or electric field [25–28]. Through fabricating different structures, diverse deformation modes in LCEs actuated by different

---

* Corresponding author at: Materials Science and Engineering Program, University of California, San Diego, La Jolla, CA 92093, USA.
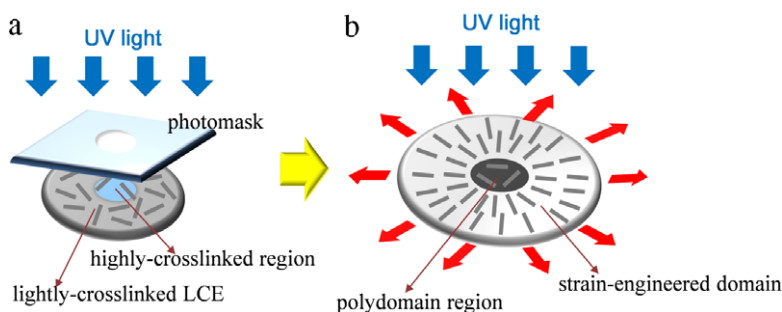*E-mail address:* shqcai@ucsd.edu (S. Cai).

Fig. 1. Schematics of the experimental steps for fabricating a patterned LCE sheet. (a) UV light is shed onto a LCE sheet through a designed photomask. When the region is exposed to UV light, second-step crosslinking reaction proceeds in the elastomer and the region becomes dramatically stiffer. (b) Subsequently, the LCE sheet is radially stretched under the exposure of UV light. Due to the material inhomogeneity, the stretch field in the LCE sheet is inhomogeneous and anisotropic, so the orientation of LC molecules in the LCE is patterned. The orientation field of LC molecules is frozen in the LCE through the second-step crosslinking reaction activated by the UV light.

stimuli have been observed in experiments [29–31]. For instance, bending, twisting or surface wrinkling in a bi-layered LCE have been realized by changing temperature [32,33]. As another example, LCEs containing photo-sensitive azobenzene moiety show three-dimensional photoactuated deformation under the light irradiation [34–36].

Recently, photoalignment method has been developed to obtain pre-designed LC molecular orientation field in LCEs [37]. Different from fabricating LCE structures with different geometries, this method directly manipulates LC molecular orientation in a LCE using properly designed light or electric field. The developed experimental method has opened not only new research opportunities but also innovative applications of LCEs [38,39]. However, the corresponding experimental setup is usually complex and the method only work for synthesizing LCEs containing several particular kinds of LC molecules.

Within the context, in the paper, we develop a strain engineering technique to pattern LC molecular orientation in LCEs. Our method can be regarded as generalization of the experiment developed by Finkelmann et al. Instead of applying homogeneous stretch, we apply predesigned inhomogeneous and anisotropic stretch in a lightly-crosslinked LCE sample, which will result in patterned LC molecular orientation. The LC molecular orientation field will be further frozen by second-step crosslinking reaction in the LCE. Our method will be generally applicable to making LCEs with different chemistries and shapes. In the letter, we will use one example: radially patterned LCE, to illustrate our ideas. We further show that different undulation in the patterned LCE sheets can be induced by thermal actuation and solvent penetration.

2. Experiment

2.1. Materials

LC monomer, 1,4-Bis-[4-(3-acryloyloxypropyloxy) benzoyloxy]-2-methylbenzene (95%, RM257) was purchased from Wilshire Technologies. Crosslinker, pentaerythritol-tetrakis(3-mercaptopropionate) (95%, PETMP) and spacer, 2,2′-(ethylenedioxy) diethanethiol (95%, EDDET), were purchased from Aldrich. Michael addition catalyst,

dipropyl amine (98%, DPA) and the photoinitiator, (2-hydroxyethoxy)-2-methylpropiophenone (98%, HHMP) were purchased from Aldrich. All chemicals were used as received without any purification.

2.2. Synthesis of a radially aligned LCE

We followed the two-step crosslinking reaction method to prepare LCE recently developed by Yakacki et al. [23]. RM257 (LC monomer) and thiol monomers, PETMP (crosslinker) and EDDET (spacer) were dissolved in toluene by heating and vigorous mixing. The molar functionality composition of thiol monomers, PETMP and EDDET was fixed as 2:8 while that between thiol monomers and RM257 was fixed as 1:1.15, so that there was 15% excess molar functional group of RM257 to that of PETMP and EDDET. A value of 0.5 wt% of HHMP to RM257 and thiol monomers, and 1.1 wt% of DPA to thiol monomers were added in the solution. After the solution was homogeneously mixed, it was placed in the vacuum chamber to remove bubbles trapped inside the solution. The solution was transferred to the mold and left overnight at room temperature for the first-step reaction. During the first step reaction, RM257 reacted with PETMP and EDDET through thiol-acrylate Michael addition to form lightly-crosslinked polydomain LCE sheet. The polydomain LCE was ready for applying mechanical stretch and second-step crosslinking reaction after the complete evaporation of toluene at 80 °C. In our experiment, the thickness of the LCE sheet after the first-step crosslinking reaction was 0.9 mm.

Orientation of LC molecules at a material point in a LCE depends on its stretch state. Qualitatively speaking, LC molecules tend to orient toward the direction with the largest tensile stretch as predicted by most models and demonstrated in experiments [40–42]. In the experiment, we generate inhomogeneous and anisotropic stretch in a LCE sheet by introducing stiff regions with different shapes into it as shown in Fig. 1.

To make a region in a lightly-crosslinked LCE sheet stiffer, we shed UV light onto a free-standing LCE sheet through a designed photomask as shown in Fig. 1. Under the UV light exposure, second-step crosslinking reaction proceeds and the region becomes dramatically stiffer. Subsequently, we manually stretch the LCE sheet in radial
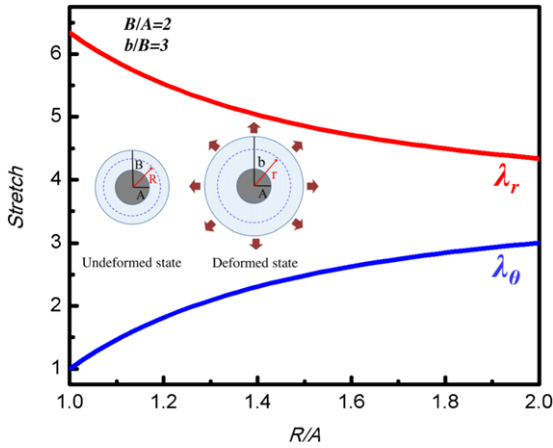
Fig. 2. Stretch distribution in a radially stretched circular LCE sheet with a stiff circular region in the middle.

directions and fix the stretch field under the exposure of UV light. Due to the material inhomogeneity, the stretch field in the LCE sheet is inhomogeneous and anisotropic, so the LC molecular orientation in the LCE will also be inhomogeneous. In the second-step crosslinking step, UV light is generated by an 8 W UV lamp with the wavelength of 365 nm. The LCE sample is placed 10 cm away from the UV lamp for 10 min.

3. Results and discussion

3.1. Inhomogeneous stress/stretch-induced patterning of LC molecular orientation

As described in Section 2, we radially stretch a lightly-crosslinked LCE sheet with a stiff region in the middle to orient LC molecules in the elastomer. Under the exposure of UV light, second-step crosslinking reaction proceeds in the stressed LCE and the patterned LC molecules are frozen in the elastomer.

The pattern formation of LC molecules under the stretch can be qualitatively understood as following: We assume the stiff region deform negligibly when the LCE is stretched. Due to the constraint, the stretch along the hoop direction of the stiff region is close to one, while the stretch perpendicular to the edge of the stiff region can be much larger than one. Therefore, regardless of the shape of the stiff region, the LC molecules near the stiff region will be perpendicular to its edge. In the area far away from the stiff region, the stretch in the LCE will be close to the far-field stretch state. Therefore, by controlling the shape of the stiff region, we can obtain different patterns of LC molecules in a LCE.

Next, as an example, we quantitatively calculate the stretch distribution in a circular LCE sheet with a circular constraint in the middle. In the undeformed state, the radius of the LCE sheet is denoted by B and the radius of the circular constraint is denoted by A (see the inset of Fig. 2). We assume the circular constraint is much stiffer than the LCE with only the completion of first-step crosslinking reaction. Therefore, after stretch, the radius of the sheet becomes b while the circular constraint remains the same. A material point in the undeformed state with the distance R from the center moves to the position with r away from the center in the deformed state. Considering the radially symmetric deformation, we can calculate the radial stretch $\lambda_r(R)$ and hoop stretch $\lambda_\theta(R)$ by
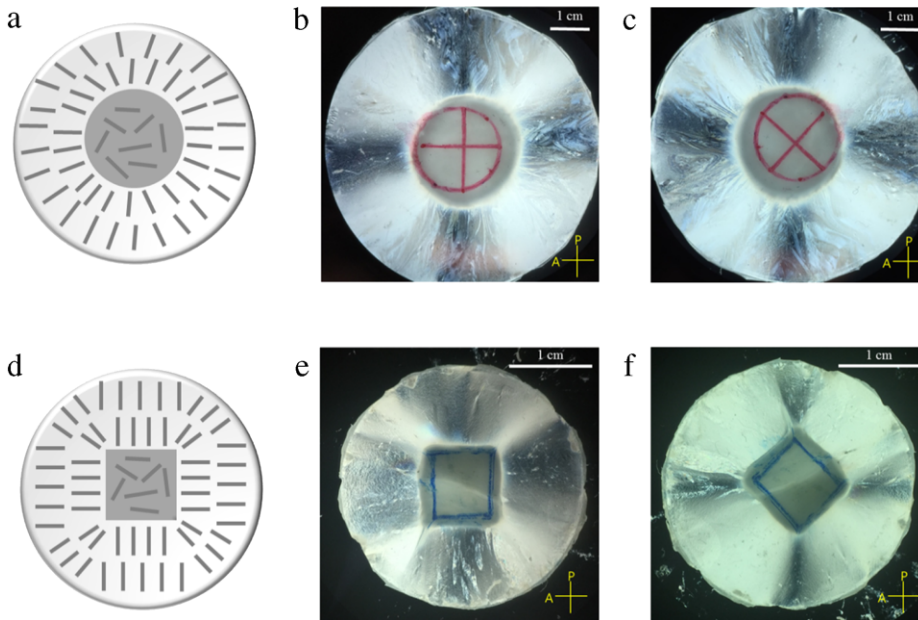
$$\lambda_r = \frac{dr}{dR}, \tag{1}$$

Fig. 3. (a) Schematic of LC molecular orientation in the LCE sheet with a circular stiff region in the middle. (b) and (c) are polarized optical microscope images of the LCE sheet with two different angles with respect to the analyzer. (d) Schematic of LC molecular orientation in the LCE sheet with a square stiff region in the middle. (e) and (f) are polarized optical microscope images of the LCE sheet with two different angles with respect to the analyzer.

$$\lambda_\theta = \frac{r}{R}. \tag{2}$$

The stress perpendicular to the LCE sheet is zero. Assuming the elasticity of the LCE can be captured by Neo-hookean model, we have the following stress–stretch relationship,

$$S_r = \mu \left(\lambda_r - \frac{1}{\lambda_r^3 \lambda_\theta^2} \right), \tag{3}$$

$$S_\theta = \mu \left(\lambda_\theta - \frac{1}{\lambda_r^2 \lambda_\theta^3} \right) \tag{4}$$

where S_r and S_θ are nominal stresses in radial and hoop direction respectively, and μ is small deformation shear modulus.

The Force balance in the radial direction is

$$\frac{dS_r}{dR} + \frac{S_r - S_\theta}{R} = 0. \tag{5}$$

A combination of Eqs. (1)–(5) gives a second order ordinary differential equation of $r(R)$. The two boundary conditions of the ODE are:

$$r(A) = A, \tag{6}$$
$$r(B) = b. \tag{7}$$

Using *Matlab*, we numerically solve the ODE. The numerical results are shown in Fig. 2. In the calculation, we set $B/A = 2$ and $b/B = 3$, which are close to our experimental conditions. From Fig. 2, we can clearly see that the radial stretch is several times larger than the hoop stretch in the area close to the edge of the constraint. The two stretches gradually get closer to each other when the area is far away from the edge of the constraint, which is due to the radial stretch applied in far field. Therefore, the LC molecules will align along the radial direction of the LCE sheet as sketched in Fig. 3(a).

Due to the optical birefringence of LC molecules, the pattern of LC molecules sketched in Fig. 3(a) can be confirmed by taking polarized optical microscope (POM) images as shown in Fig. 3(b) and (c). In Fig. 3(b), the pattern with maximum brightness can be observed at around 45° with respect to the analyzer while the darkest pattern at around 0° and 90°. In Fig. 3(c), the POM image of the LCE rotated by 45° with respect to its original position is very similar to that in Fig. 3(b). It is known that the maximum light transmittance can be found when the LC molecule is 45° between crossed polarizer and analyzer [43]. Therefore, we can confirm that LC molecules in the LCE are indeed along its radial direction as sketched in Fig. 3(a).

To examine the effects of the shape of the constraint, we also introduced a stiff region with square shape in the LCE sheet. As discussed at the beginning of this section, LC molecules will align perpendicular to the edge of the stiff region when the LCE sheet is radially stretched in far field. Fig. 3(d) sketches the LC molecular patterns. Similarly, the expected LC molecular patterns are confirmed by the POMs of the LCE sheet at different rotational angle as shown in Fig. 3(e) and (f). Different patterns shown in Fig. 3(a) and (d) are caused by the different shape of the stiff region: circular and square. The results clearly indicate that our
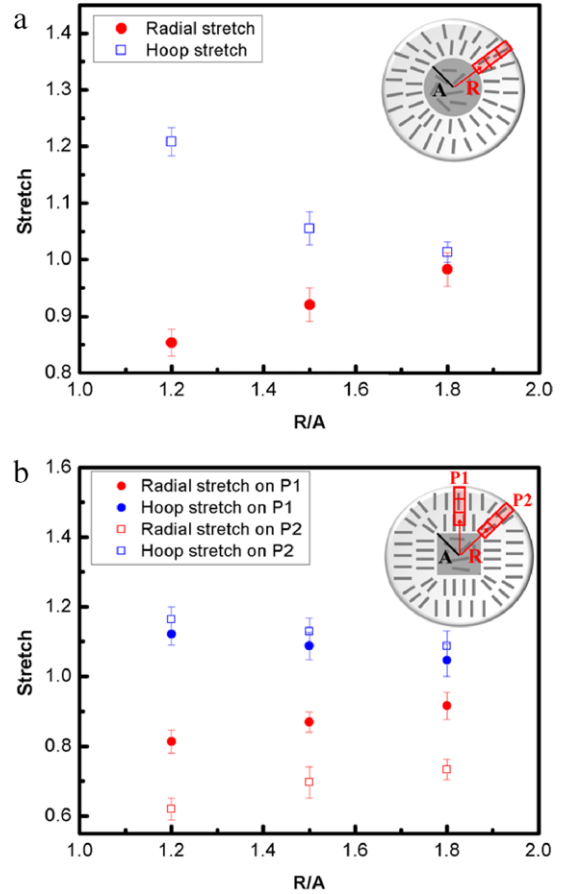

Fig. 4. Thermally-actuated radial and hoop stretch on the patterned LCEs along radial directions with different distances away from the constraint. (a) Three LCE samples cut from an arbitrary radial path in a patterned LCE sheet with a circular constraint. (b) LCE samples cut from two different radial paths: P1 and P2 from a patterned LCE with a square constraint.

experimental method can be readily used to obtain diverse LC molecular patterns through introducing stiff constraints with different shapes into the LCE.

As shown in Fig. 2, the stretch of the material point near the constraint is more anisotropic than the one close to the free edge. Therefore, the orientation of LC molecules in the LCE is not only anisotropic but also inhomogeneous along the radial direction. More specifically, the LC molecules in the LCE near the constraint should be more aligned than the molecules far away from the constraint.

To confirm the above assumption, we further conduct thermal-actuation experiments in the patterned LCE sample. In the experiment, we cut three small square LCE samples from two patterned LCE sheets with different constraint shapes along the radial direction with different distances away from the constraint as shown in the inset figure of Fig. 4(a) and (b). As expected, upon being heated up to 80 °C, all the three square LCE samples contract parallel to the direction of LC molecular orientation (radial direction) while expand in the perpendicular direction (hoop direction).

Fig. 4(a) plots the radial and hoop stretches of three square LCE samples from a patterned LCE sheet with a circular constraint. Because the LCE sheet is asymmetric, we
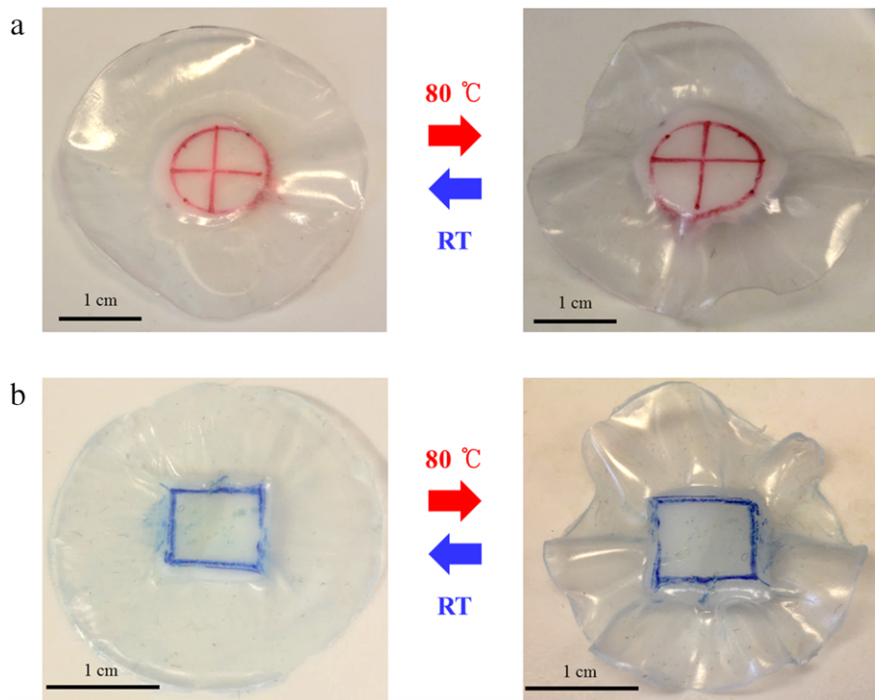
Fig. 5. Reversible thermally driven undulation in patterned LCEs with a (a) circular constraint and (b) square constraint in the middle.

cut the three square LCE samples from an arbitrary radial path in the LCE sheet in the experiment. Fig. 4(b) plots the radial and hoop stretches of three square LCE samples from a patterned LCE sheet with a square constraint. For the patterned LCE sheet with a square constraint, as shown in the inset figure of Fig. 4(b), we cut the three LCE samples from two different radial paths, P1 and P2: P1 is from the center of square and perpendicular to an edge of the square constraint; P2 is along the connection between the center of the square and its vertex. The results in Fig. 4(a) and (b) clearly show that the LCE sample near the constraint has the maximum anisotropy of thermal-actuated strain, while the LCE sample near the free edge has the minimal anisotropy. The experimental results confirm our assumption that the LC molecules in the LCE near the constraint are more aligned than the molecules far away from the constraint. In addition, Fig. 4(b) also shows that, for the patterned LCE sheet with a square constraint, the anisotropy of thermal-actuated strain along the radial path passing through the square vertex is generally larger than the one in the radial path perpendicular to the edge of the square. This is the consequence of stress concentration caused by the sharp vertex of the square.

3.2. Reversible undulation in patterned LCEs driven by temperature variation and solvent penetration

Because LC molecules tend to be more and more randomly orientated with increasing temperature, upon being heated up, a patterned LCE will contract along the direction of LC molecular orientation while expand in the perpendicular direction as shown in Fig. 4. In the experiment, when a flat patterned LCE sheet is heated up,

due to the anisotropic actuation, multiple wrinkles form in the LCE sheet as shown in Fig. 5. In the experiment, we place the patterned LCE film on a hot plate with the temperature 80 °C, which is above the phase transition temperature of the LCE we synthesized. Multiple wrinkles appear in the patterned LCE film within a few seconds (Fig. 5(a) and (b)).

To quantitatively investigate the wrinkling instability induced by the temperature change, we further measure the winkling amplitude in a patterned LCE sheet at different temperatures as shown in Fig. 6. In the exper-
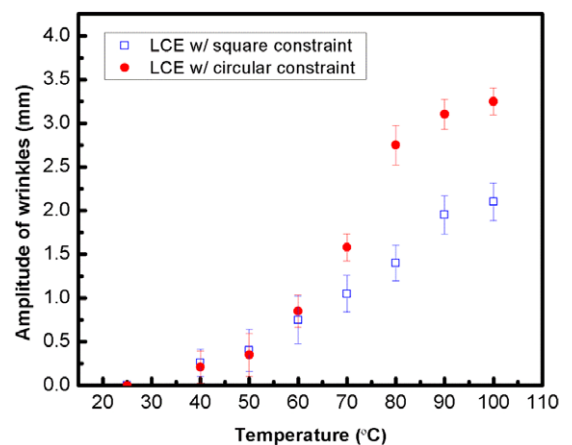

Fig. 6. Evolution of the amplitude of wrinkles with the increase of temperature. For the LCE with a circular constraint, the amplitudes of different wrinkles are the same. For the LCE with a square constraint, we measure the amplitude of the wrinkle, which is perpendicular to the edge of the square.
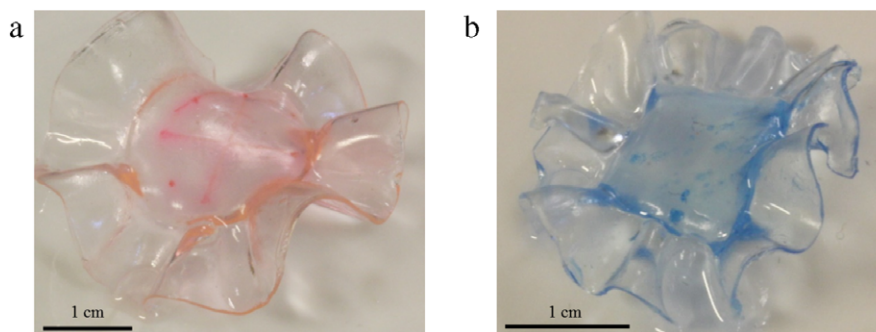
Fig. 7. Solvent penetration driven undulation in patterned LCEs with a (a) circular constraint and (b) square constraint in the middle.

iment, with increasing the temperature, the amplitude of wrinkles in the patterned LCE sheets increases while the wavenumber does not change. Fig. 6 shows that a noticeable wrinkling deformation can be observed in the experiment around 40 °C for both the LCE sheets with a circular constraint or square constraint. With different patterns of LC molecules, the wrinkling morphologies driven by temperature change are also different in the LCE sheets as shown in Fig. 5(a) and (b). We would like to further point out that the mechanism of generating the undulation in the LCE sheet is different from that of the formation of wrinkles in a circular gel sheet undergoing inhomogeneous swelling [44,45]. The size of the LCE sheet reduces about 15% when the temperature increases as shown in Fig. 5(a) and (b). In addition, when we remove the undulated LCE film from the hot plate to another plate with room temperature, the LCE sheet can fully recover back to flat shape within several seconds.

A patterned LCE also swells anisotropically in a solvent. When a patterned LCE is submerged into a solvent such as toluene, its swelling ratio along the direction of LC molecular orientation is much smaller than the perpendicular to the direction of LC molecular orientation [22]. Therefore, similar undulating deformation in the patterned LCE sheets can be also driven by solvent penetration as shown in Fig. 7. The undulated LCE sheets can also recover to its original flat shape after it is dried out.

4. Conclusions

In recent years, programmable soft materials and structures have been intensively studied. The material includes hydrogels, shape memory polymers and biopolymers. In the letter, we developed a facile and effective strain engineering technique to pattern LC molecules in a LCE. As a result, the patterned LCE can have different active deformation modes when subjected to various external stimuli, and thus realize different functions. Although only simple patterns in LCE sheets have been demonstrated in the letter, there should not be any intrinsic difficulties to generate more complex LC molecular patterns in a LCE by applying inhomogeneous stretch. We believe the strain engineering technique developed in the article can be directly used to fabricate programmable LCE structures, which is the ongoing research being conducted by us.

References

[1] S. Dey, D. Agra-Kooijman, W. Ren, P. McMullan, A. Griffin, S. Kumar, Soft elasticity in main chain liquid crystal elastomers, Crystals 3 (2) (2013) 363.

[2] J.S. Biggins, M. Warner, K. Bhattacharya, Elasticity of polydomain liquid crystal elastomers, J. Mech. Phys. Solids 60 (4) (2012) 573–590.

[3] A.W. Brown, J.M. Adams, Negative Poisson's ratio and semisoft elasticity of smectic-C liquid-crystal elastomers, Phys. Rev. E 85 (1) (2012) 011703.

[4] J.M. Adams, M. Warner, Soft elasticity in smectic elastomers, Phys. Rev. E 72 (1) (2005) 011703.

[5] D. Corbett, M. Warner, Changing liquid crystal elastomer ordering with light—a route to opto-mechanically responsive materials, Liq. Cryst. 36 (10–11) (2009) 1263–1280.

[6] N.J. Dawson, M.G. Kuzyk, J. Neal, P. Luchette, P. Palffy-Muhoray, Modeling the mechanisms of the photomechanical response of a nematic liquid crystal elastomer, J. Opt. Soc. Amer. B 28 (9) (2011) 2134–2141.

[7] H. Finkelmann, M. Shahinpoor, Electrically-controllable liquid crystal elastomer-graphite composite artificial muscles, in: Smart Structures and Materials 2002: Electroactive Polymer Actuators and Devices, Eapad, 4695, 2002, pp. 459–464.

[8] S. Petsch, R. Rix, P. Reith, B. Khatri, S. Schuhladen, D. Ruh, R. Zentel, H. Zappe, A thermotropic liquid crystal elastomer micro-actuator with integrated deformable micro-heater, in: 2014 IEEE 27th International Conference on Micro Electro Mechanical Systems, MEMS, p. 905.

[9] H. Xing, J. Li, J. Guo, J. Wei, Bio-inspired thermal-responsive inverse opal films with dual structural colors based on liquid crystal elastomer, J. Mater. Chem. C 3 (17) (2015) 4424–4430.

[10] M.H. Li, P. Keller, Artificial muscles based on liquid crystal elastomers, Phil. Trans. R. Soc. A-Math. Phys. Eng. Sci. 364 (2006) 2763–2777.

[11] J. Schmidtke, S. Kniesel, H. Finkelmann, Probing the photonic properties of a cholesteric elastomer under biaxial stress, Macromolecules 38 (4) (2005) 1357–1363.

[12] J. Schmidtke, W. Stille, H. Finkelmann, S.T. Kim, Laser emission in a dye doped cholesteric polymer network, Adv. Mater. 14 (10) (2002) 746–749.

[13] N.J. Dawson, M.G. Kuzyk, J. Neal, P. Luchette, P. Palffy-Muhoray, Cascading of liquid crystal elastomer photomechanical optical devices, Opt. Commun. 284 (4) (2011) 991–993.

[14] S.V. Shilov, H. Skupin, F. Kremer, K. Skarp, P. Stein, H. Finkelmann, Segmental motion of ferroelectric liquid crystal polymer and elastomer during electro-optical switching, pp. 62–67.

[15] P. Dalhaimer, D.E. Discher, T.C. Lubensky, Crosslinked actin networks show liquid crystal elastomer behaviour, including soft-mode elasticity, Nat. Phys. 3 (5) (2007) 354–360.

[16] D.P. Knight, F. Vollrath, Biological liquid crystal elastomers, Philos. Trans. R. Soc. B 357 (1418) (2002) 155–163.

[17] C. Li, Y. Liu, C.-w. Lo, H. Jiang, Reversible white-light actuation of carbon nanotube incorporated liquid crystalline elastomer nanocomposites, Soft Matter 7 (16) (2011) 7511–7516.

[18] K. Urayama, S. Honda, T. Takigawa, Deformation coupled to director rotation in swollen nematic elastomers under electric fields, Macromolecules 39 (5) (2006) 1943–1949.

[19] A. Agrawal, A.C. Chipara, Y. Shamoo, P.K. Patra, B.J. Carey, P.M. Ajayan, W.G. Chapman, R. Verduzco, Dynamic self-stiffening in liquid crystal elastomers, Nature Commun. 4 (2013) 1739.

[20] H. Schüring, R. Stannarius, C. Tolksdorf, R. Zentel, Liquid crystal elastomer balloons, Macromolecules 34 (12) (2001) 3962–3972.

[21] R. Diaz-Calleja, P. Llovera-Segovia, E. Riande, A. Quijano López, Mechanic and electromechanic effects in biaxially stretched liquid crystal elastomers, Appl. Phys. Lett. 102 (5) (2013) 052901.

[22] J. Küpfer, H. Finkelmann, Nematic liquid single crystal elastomers, Die Makromol. Chem. Rapid Commun. 12 (12) (1991) 717–726.

[23] C.M. Yakacki, M. Saed, D.P. Nair, T. Gong, S.M. Reed, C.N. Bowman, Tailorable and programmable liquid-crystalline elastomers using a two-stage thiol-acrylate reaction, RSC Adv. 5 (25) (2015) 18997–19001.

[24] F. Brömmel, D. Kramer, H. Finkelmann, Preparation of liquid crystalline elastomers, in: W.H. de Jeu (Ed.), Liquid Crystal Elastomers: Materials and Applications, Springer, Berlin, Heidelberg, 2012, pp. 1–48.

[25] W. Lehmann, H. Skupin, C. Tolksdorf, E. Gebhard, R. Zentel, P. Kruger, M. Losche, F. Kremer, Giant lateral electrostriction in ferroelectric liquid-crystalline elastomers, Nature 410 (6827) (2001) 447–450.

[26] T. Ikeda, M. Nakano, Y. Yu, O. Tsutsumi, A. Kanazawa, Anisotropic bending and unbending behavior of azobenzene liquid-crystalline gels by light exposure, Adv. Mater. 15 (3) (2003) 201–205.

[27] N. Torras, K.E. Zinoviev, J. Esteve, A. Sanchez-Ferrer, Liquid-crystalline elastomer micropillar array for haptic actuation, J. Mater. Chem. C 1 (34) (2013) 5183–5190.

[28] M. Brehmer, R. Zentel, Ferroelectric liquid-crystalline elastomers with short switching times, Macromol. Rapid Commun. 16 (9) (1995) 659–662.

[29] C. Ohm, M. Brehmer, R. Zentel, Liquid crystalline elastomers as actuators and sensors, Adv. Mater. 22 (31) (2010) 3366–3387.

[30] M. Yamada, M. Kondo, R. Miyasato, Y. Naka, J.-i. Mamiya, M. Kinoshita, A. Shishido, Y. Yu, C.J. Barrett, T. Ikeda, Photomobile polymer materials-various three-dimensional movements, J. Mater. Chem. 19 (1) (2009) 60–62.

[31] Y. Yu, M. Nakano, T. Ikeda, Photomechanics: Directed bending of a polymer film by light, Nature 425 (6954) (2003) 145.

[32] A. Agrawal, T. Yun, S.L. Pesek, W.G. Chapman, R. Verduzco, Shape-responsive liquid crystal elastomer bilayers, Soft Matter 10 (9) (2014) 1411–1415.

[33] A. Agrawal, P. Luchette, P. Palffy-Muhoray, S.L. Biswal, W.G. Chapman, R. Verduzco, Surface wrinkling in liquid crystal elastomers, Soft Matter 8 (27) (2012) 7138–7142.

[34] T. Yoshino, M. Kondo, J.-i. Mamiya, M. Kinoshita, Y. Yu, T. Ikeda, Three-dimensional photomobility of crosslinked azobenzene liquid-crystalline polymer fibers, Adv. Mater. 22 (12) (2010) 1361–1363.

[35] R. Yin, W. Xu, M. Kondo, C.-C. Yen, J.-i. Mamiya, T. Ikeda, Y. Yu, Can sunlight drive the photoinduced bending of polymer films? J. Mater. Chem. 19 (20) (2009) 3141–3143.

[36] S. Iamsaard, S.J. Aßhoff, B. Matt, T. Kudernac, J.L.M. Cornelissen Jeroen, S.P. Fletcher, N. Katsonis, Conversion of light into macroscopic helical motion, Nat. Chem. 6 (3) (2014) 229–235.

[37] T. Seki, New strategies and implications for the photoalignment of liquid crystalline polymers, Polym. J. 46 (11) (2014) 751–768.

[38] T.H. Ware, M.E. McConney, J.J. Wie, V.P. Tondiglia, T.J. White, Voxelated liquid crystal elastomers, Science 347 (6225) (2015) 982–984.

[39] L.T. de Haan, C. Sánchez-Somolinos, C.M.W. Bastiaansen, A.P.H.J. Schenning, D.J. Broer, Engineering of complex order and the macroscopic deformation of liquid crystal polymer networks, Angew. Chem. Int. Ed. 51 (50) (2012) 12469–12472.

[40] Z. Wei, S. Michael, P. Peter, Modeling and simulation of liquid-crystal elastomers, Phys. Rev. E 83 (5) (2011) 051703.

[41] P. Bladon, E.M. Terentjev, M. Warner, Transitions and instabilities in liquid crystal elastomers, Phys. Rev. E 47 (6) (1993) R3838–R3840.

[42] S. Conti, A. DeSimone, G. Dolzmann, Soft elastic response of stretched sheets of nematic elastomers: a numerical study, J. Mech. Phys. Solids 50 (7) (2002) 1431–1451.

[43] A. Komp, J. Rühe, H. Finkelmann, A versatile preparation route for thin free-standing liquid single crystal elastomers, Macromol. Rapid Commun. 26 (10) (2005) 813–818.

[44] J. Kim, J.A. Hanna, M. Byun, C.D. Santangelo, R.C. Hayward, Designing responsive buckled surfaces by halftone gel lithography, Science 335 (6073) (2012) 1201–1205.

[45] Z. Liu, S. Swaddiwudhipong, W. Hong, Pattern formation in plants via instability theory of hydrogels, Soft Matter 9 (2) (2013) 577–587.